

Boosting the power factor with resonant states: A model study

S. Thébaud,* Ch. Adessi, S. Pailhès, and G. Bouzerar

Université de Lyon, Université Claude Bernard Lyon 1 and CNRS, Institut Lumière Matière, F-69622 Lyon, France

(Received 27 April 2017; published 1 August 2017)

A particularly promising pathway to enhance the efficiency of thermoelectric materials lies in the use of resonant states, as suggested by experimentalists and theorists alike. In this paper, we go over the mechanisms used in the literature to explain how resonant levels affect the thermoelectric properties, and we suggest that the effects of hybridization are crucial yet ill understood. In order to get a good grasp of the physical picture and to draw guidelines for thermoelectric enhancement, we use a tight-binding model containing a conduction band hybridized with a flat band. We find that the conductivity is suppressed in a wide energy range near the resonance, but that the Seebeck coefficient can be boosted for strong enough hybridization, thus allowing for a significant increase of the power factor. The Seebeck coefficient can also display a sign change as the Fermi level crosses the resonance. Our results suggest that in order to boost the power factor, the hybridization strength must not be too low, the resonant level must not be too close to the conduction (or valence) band edge, and the Fermi level must be located around, but not inside, the resonant peak.

DOI: [10.1103/PhysRevB.96.075201](https://doi.org/10.1103/PhysRevB.96.075201)**I. INTRODUCTION**

The prospect of an unprecedented global crisis, due to our energy dependence toward unclean fossil resources such as oil and coal, has led to a tremendous push in research for clean and sustainable energy sources. Consequently, there has been a renewed interest toward thermoelectric materials in the field of condensed matter physics [1,2]. Thermoelectric generators that could be competitive on an industrial scale require [1,3–5] thermoelectric materials exhibiting a large figure of merit zT , defined as

$$zT = \frac{\sigma S^2}{\kappa} T,$$

in which σ is the electrical conductivity, S the Seebeck coefficient, κ the thermal conductivity, and T the temperature. The higher zT is, the closer the device efficiency is to the Carnot efficiency. In the past decades, the drive to develop efficient thermoelectric devices has led scientists to search for green and industry-friendly materials exhibiting a figure of merit of at least 1. The standard procedure for boosting zT has been to decrease the thermal conductivity by using alloyed, nanostructured, or nanocomposite materials [6–9]. However, there is a growing concern that this method will soon reach its limits and that further significant progress will be achieved by focusing on the power factor σS^2 .

Hicks and Dresselhaus breathed new life into the field when they theorized that the electronic part of the figure of merit could be greatly enhanced by spatially confining known thermoelectric materials in two-dimensional quantum wells [10] or in one-dimensional quantum wires [11]. These papers gave rise to a great drive towards the synthesis of materials exhibiting a reduction of dimensionality [12–14], by trapping electrons either in superlattices, for instance, PbTe/Pb_{1-x}Eu_xTe [15] and Bi₂Te₃/Sb₂Te₃ [16], or in the interface between two compounds, such as TiO₂ and SrTiO₃ [17]. The basic idea is to increase the density of state (DOS) near the band edge in order to boost the power factor. A few years later, Mahan and

Sofa [18] suggested a mechanism by which the introduction of a sharp peak in the DOS could significantly boost the figure of merit. This can be achieved by doping a bulk compound with a dopant that creates sharp hybridized impurity states inside the conduction or valence band of the host material: such states are called resonant states or virtual bound states. A great virtue of this method is its applicability to both thin films and bulk materials, unlike electronic confinement which usually requires thin films. The procedure has been attempted by many researchers (see the review by Heremans *et al.* [19]), for instance in the case of thallium-doped PbTe [20,21], tin-doped Bi₂Te₃ [22], indium-doped SnTe [23,24], or aluminium-doped PbSe [25]. It has also been suggested [18] that the very high power factor of YbAl₃ [26,27] could be explained by the presence of a sharp f -level peak in its DOS [28]. On the theoretical side, the calculation of thermoelectric transport properties is most often achieved by using first-principle density functional theory simulations and the Boltzmann equation under the constant relaxation time approximation, methods that are material specific and often quite demanding in computation time [29–33].

Despite such intense activity around resonant states in thermoelectricity, there are still a few widespread misconceptions about how resonant levels affect thermoelectric transport. In this paper, our aim is to put forward a clear physical picture and provide a few guidelines to best achieve a resonant enhancement of the power factor. In the second part, we discuss the mechanisms as presented in most of the existing literature and point out their limitations. In a third part, we present an alternative physical picture with the help of a simple tight-binding model. This model allows us to identify some important trends and the role of the main physical parameters, independently of any material-specific band structure or scattering law.

II. THE TRANSPORT DISTRIBUTION FUNCTION

The electronic transport properties of any compound depend on a single material-dependent function of the energy and the temperature, called the transport distribution function (TDF) $\Sigma(E, T)$. Once the TDF is known, the electrical

*simon.thebaud@univ-lyon1.fr

conductivity σ and the Seebeck coefficient S at a given temperature T and temperature-dependent chemical potential $\mu(T)$ can be obtained as [34]

$$\sigma(T) = \int dE \left(-\frac{\partial f}{\partial E} \right) \Sigma(E, T), \quad (1)$$

$$S(T) = -\frac{1}{eT\sigma} \int dE \left(-\frac{\partial f}{\partial E} \right) (E - \mu) \Sigma(E, T), \quad (2)$$

in which e is the elementary charge and f the Fermi distribution. Since $(-\frac{\partial f}{\partial E})$ is basically a window function of width $\approx 4k_B T$ centered on μ , these relations simplify at low temperature to

$$\sigma(T) \approx \Sigma(E = \mu, T), \quad (3)$$

$$S(T) \approx -\frac{\pi^2 k_B^2 T}{3e} \frac{1}{\Sigma} \frac{\partial \Sigma}{\partial E} (E = \mu, T), \quad (4)$$

which are the well-known Mott formula [4,34]. Therefore, to maximize the power factor σS^2 , one needs to find a material in which the TDF has a high amplitude (high conductivity) as well as sharp variations (high Seebeck coefficient).

Mahan and Sofo [18] found that the shape of the TDF most conducive to good thermoelectric properties is the delta function. Writing the Einstein formula [34]

$$\Sigma(E, T) = e^2 g(E) v_x^2(E) \tau(E, T), \quad (5)$$

in which $g(E)$ is the DOS, $v_x(E)$ is the band velocity along the transport direction x , and $\tau(E, T)$ is the relaxation time, they suggested that a sharp peak in the DOS would translate to a sharp peak in the TDF [Fig. 1(a)], provided that the velocity v_x is not suppressed significantly around resonance (as we will see, the velocity is actually strongly affected in most cases, the picture of Fig. 1(a) is therefore usually invalid). In this case, they also calculated that the presence of a background DOS could destroy the resonant effect, which would encourage looking for resonant states very near the host valence or conduction band edge. Notice how the sign of the slope of the TDF changes around the resonant state in this physical picture. Consequently, one should expect the sign of the Seebeck coefficient to change as the Fermi level crosses the resonant band. This interpretation has been invoked to explain the results of *ab initio* calculations for ZnSe containing O impurities [35].

Another slightly different mechanism is used to explain the effects of resonant states throughout the literature [19,20,25,36]. Since the TDF is basically the conductivity at

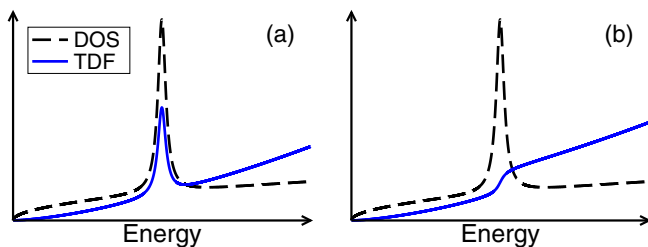


FIG. 1. Schematic representation of the density of state (dashed black line) and transport distribution function (solid blue line) in the presence of a resonant peak, in the Mahan-Sofo picture (a) and in the “carrier density” picture (b).

low temperature, one can write

$$\Sigma(E, T) \approx en(E)\mu_x(E, T), \quad (6)$$

in which $n(E)$ is the total carrier density and $\mu_x(E, T)$ is the carrier mobility along the transport direction. The Mott formula then yields

$$S \approx -\frac{\pi^2 k_B^2 T}{3e} \left(\frac{1}{n} \frac{\partial n}{\partial E} + \frac{1}{\mu_x} \frac{\partial \mu_x}{\partial E} \right). \quad (7)$$

The first term, $\frac{1}{n} \frac{\partial n}{\partial E} = \frac{g(E)}{n(E)}$, depends very little on temperature and is associated with band structure effects; it is straightforward to see that a local increase in the DOS would cause a local boost in the Seebeck coefficient. The second term, $\frac{1}{\mu_x} \frac{\partial \mu_x}{\partial E}$, is associated in the literature with scattering. If the resonant states bring about a drastic change in the carrier scattering, the Seebeck coefficient might be boosted through this term. The effects of resonant scattering are thought to vanish at high temperature, as the scattering becomes dominated by phonons. Therefore, this mechanism is probably unable to help in designing materials for power generation (which usually involves high temperatures) and is not the topic of this paper which is focused on band structure effects. Assuming no resonant scattering, then, the carrier mobility is thought not to change violently around the resonance, and the TDF is approximately proportional to the carrier density n [Fig. 1(b)]. Note that in this picture, the slope of the TDF remains positive, so the sign of the Seebeck coefficient is not expected to change. Moreover, the Fermi level should be located right at the resonance for maximum effect.

Both mechanisms in Fig. 1 require the resonant states to participate in conduction, meaning that either the band velocity v_x or the mobility μ_x must not be drastically suppressed by the resonance. This seems incompatible with the requirement that the resonant peak in the DOS be sharp since a flat band implies low velocities and low mobilities. The mobility is indeed not simply a scattering quantity: one can see from the Drude formula $\mu_x = e\tau/m_x^*$ that a large effective band mass m_x^* suppresses the mobility, and a flat band is precisely composed of heavy carrier states (consequently, associating the term $\frac{1}{\mu_x} \frac{\partial \mu_x}{\partial E}$ of Eq. (7) to resonant scattering only and discarding it on this ground is incorrect in many cases). Thus, a single very flat band, for instance, a doping impurity band in the gap of the host material, leads to bad thermoelectric properties despite having a very δ -like DOS [37,38]. Confinement techniques work around this problem because they introduce flat dispersions only in the confinement directions. For the same reason, highly anisotropic orbitals like d orbitals are naturally conducive to good thermoelectric properties, and it is possible to boost the power factor by making them come into play [39]. Even then, a recent study [40] clearly shows that they must have both a strong weight in the DOS and a sufficient dispersion in the transport direction to enhance the thermoelectric properties. Another technique, called band convergence [41], consists of engineering a material to add other valleys at the bottom of the conduction band or at the top of the valence band; this has been achieved, for instance, in selenium-doped PbTe [42]. The sharpness of the DOS increase is then abandoned, and the DOS is, in effect, multiplied by a factor: at fixed Fermi energy, the conductivity is increased while the Seebeck coefficient is

unchanged. However, in the case of a sharp peak in the DOS of a bulk material, which is the focus of this paper, there are two types of carrier states: light carriers, corresponding to the undistorted bands of the material, and heavy carriers, corresponding to the peak in the DOS. As noted by Heremans *et al.* [19], if the two types of states are not hybridized with one another, the transport properties are entirely dominated by the light carriers (which have the highest conductivity) and the sharp peak is useless. Therefore, some hybridization is needed to boost the power factor.

This raises a few questions: What exactly happens to the TDF when there is hybridization? What is the right hybridization strength? Where should the resonant level be, with respect to the edge of the host band? Where should the Fermi level be, with respect to the resonant level? What kind of boost can we expect for the power factor? In order to answer these questions and investigate the typical behavior of the relevant quantities independently of the material-specific band structure or scattering law, we make use of a tight-binding model containing a flat band hybridized with a conduction band. Contrary to the parabolic band model, a tight-binding description let us explore the entire band structure and thus choose freely the position of the Fermi level and the resonant band. Such tight-binding models have been shown to successfully describe the electronic structure of oxides in confinement problems [43,44] and the bulk thermoelectric properties of SrTiO₃ [45].

III. TIGHT-BINDING MODEL

In order to study the typical effects of resonant states on the thermoelectric properties in the simplest and clearest way, we write a spinless tight-binding Hamiltonian on a simple cubic lattice ($N = L^3$ sites, lattice constant a) featuring an extended conduction band and a heavy resonant band:

$$\mathcal{H} = \mathcal{H}_0 + \mathcal{H}_V, \quad (8)$$

in which

$$\mathcal{H}_0 = -t_0 \sum_{\langle \mathbf{i}, \mathbf{j} \rangle} (c_{\mathbf{i}}^\dagger c_{\mathbf{j}} + c_{\mathbf{j}}^\dagger c_{\mathbf{i}}) + E_l \sum_{\mathbf{i}} l_{\mathbf{i}}^\dagger l_{\mathbf{i}} \quad (9)$$

and \mathcal{H}_V is the hybridization term:

$$\mathcal{H}_V = V \sum_{\mathbf{i}} (c_{\mathbf{i}}^\dagger l_{\mathbf{i}} + l_{\mathbf{i}}^\dagger c_{\mathbf{i}}), \quad (10)$$

with $\langle \mathbf{i}, \mathbf{j} \rangle$ being the pairs of nearest-neighboring sites in the lattice, $c_{\mathbf{i}}$ the electron annihilation operator on the site \mathbf{i} in an extended conduction orbital, and $l_{\mathbf{i}}$ the electron annihilation operator on the site \mathbf{i} in a heavy resonant orbital. As the spin degree of freedom is irrelevant in this study, we write a spinless Hamiltonian for the sake of clarity and simply take into account the spin degeneracy by introducing a factor of 2 in our numerical results.

The first term in \mathcal{H}_0 gives rise to a conduction band (extended states) of width $12t_0$ and dispersion $\epsilon(\mathbf{k}) = -2t_0[\cos(k_x a) + \cos(k_y a) + \cos(k_z a)]$, with t_0 being the hopping constant. As there is no hopping term for the resonant orbitals, those give rise to a flat band (heavy states): the second term in \mathcal{H}_0 governs the position E_l of this flat band in the DOS. \mathcal{H}_V hybridizes the two orbitals (extended and heavy) in each

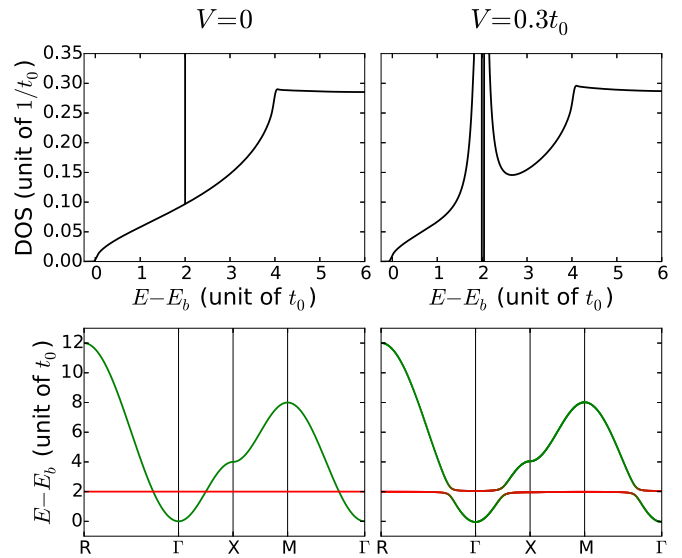


FIG. 2. DOS and dispersions for $V = 0$ (left panels) and $V = 0.3t_0$ (right panels) with $E_l - E_b = 2t_0$. E_b designates the bottom of the lower band. Green denotes the extended conduction orbital character and red denotes the heavy resonant orbital character. Different values of V yield qualitatively similar results.

lattice site, with a hybridization strength V . If $V = 0$, there is no hybridization and the heavy states do not participate in conduction at all.

Given the simplicity of this model, we do not aim in this paper to reproduce experimental results. Rather, our goal is to investigate the general consequences of hybridizing a flat band with an extended conduction band and to clarify the role of each physical parameters. Thus, we are to compare the thermoelectric transport properties in the absence of resonance (which corresponds to the reference case $V = 0$) to the same properties in the presence of hybridization (resonant case).

The Hamiltonian \mathcal{H} can be diagonalized straightforwardly. The lower half of the DOS and the two-band dispersions are plotted in Fig. 2, for $V = 0$ and $V = 0.3t_0$, with $E_l - E_b = 2t_0$ (E_b being the bottom of the conduction band). Several values for V and E_l are subsequently considered. If the orbitals are hybridized, the peak in the DOS broadens and, in this model, a hybridization gap appears.

To separate the influence of scattering in electronic transport from the effects of the band structure, we write the TDF as

$$\Sigma(E, T) = D(E) \tau(E, T), \quad (11)$$

in which $D(E)$ is the Drude weight [46,47]. The Drude weight is computed by inserting a magnetic flux ϕ along the transport direction and taking the derivative of the many-body ground-state energy E_0 :

$$D = \frac{1}{aL} \frac{\partial^2 E_0}{\partial \phi^2}. \quad (12)$$

It also satisfies the sum rule [48,49]

$$D + \frac{2}{\pi} \int_0^\infty d\omega \sigma_{\text{reg}}(\omega) = \frac{e^2 t_0}{a\hbar^2} \frac{\langle -\hat{K}_x / N \rangle}{t_0}, \quad (13)$$

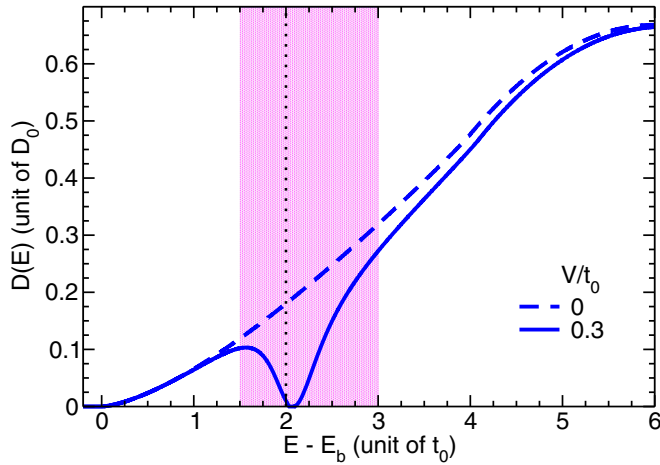


FIG. 3. Drude weight in units of $D_0 = \frac{e^2 t_0}{a \hbar^2}$ for $V = 0$ (dashed line) and for $V = 0.3t_0$ (solid line) with $E_l - E_b = 2t_0$ (a dotted vertical line marks the position of the flat band). Different values of V yield qualitatively similar results. The shading marks the zone in which the Drude weight is suppressed.

in which $\sigma_{\text{reg}}(\omega)$ is the regular part of the optical conductivity and \hat{K}_x is, in this model, the kinetic energy along the transport direction x . $D_0 = \frac{e^2 t_0}{a \hbar^2}$ is henceforth the unit of the Drude weight. For our translationally invariant Hamiltonian, the regular conductivity is associated with interband transitions and we checked that the sum rule is satisfied. As for the relaxation time, a realistic expression for τ would be highly material dependent (dominating scattering process, presence of disorder and impurities, etc.) and remember that the effects of resonant scattering are supposed to disappear at high temperature. This paper investigates the consequences on thermoelectric transport of distortions in the TDF caused through band structure effects by the presence of a resonant band. Therefore, we use the constant relaxation time approximation: $\tau = \tau_0$, with τ_0 being a constant. Consequently, the TDF is simply proportional to the Drude weight, which makes $D(E)$ the central quantity of this study. However, it is important to note that using a constant relaxation time is not always justified. Further studies investigating the effects of resonant scattering (which is beyond the scope of this paper) are needed to go above this first approximation.

The Drude weight as a function of the Fermi energy is shown in Fig. 3 for the reference case ($V = 0$) and the resonant case ($V = 0.3t_0$, $E_l - E_b = 2t_0$), in units of D_0 . For the reference case, the regular conductivity vanishes and the Drude weight identifies with the right-hand side of Eq. (13), which is a rather smooth and monotonic function of the energy. In contrast, in the resonant case, there is a substantial drop in the Drude weight within the resonant band region. This is due to the mixing of the heavy and light carriers near E_l ; the latter acquire a heavy character which drastically suppresses their conduction. It is important to compare Fig. 3 to the mechanisms represented in Fig. 1, notice how the effects of resonant states on the TDF are unlike anything proposed in the literature. Drawing the consequences for the thermoelectric properties, this result appears at first to be unfavorable. The TDF, and consequently the electrical conductivity, is strongly suppressed

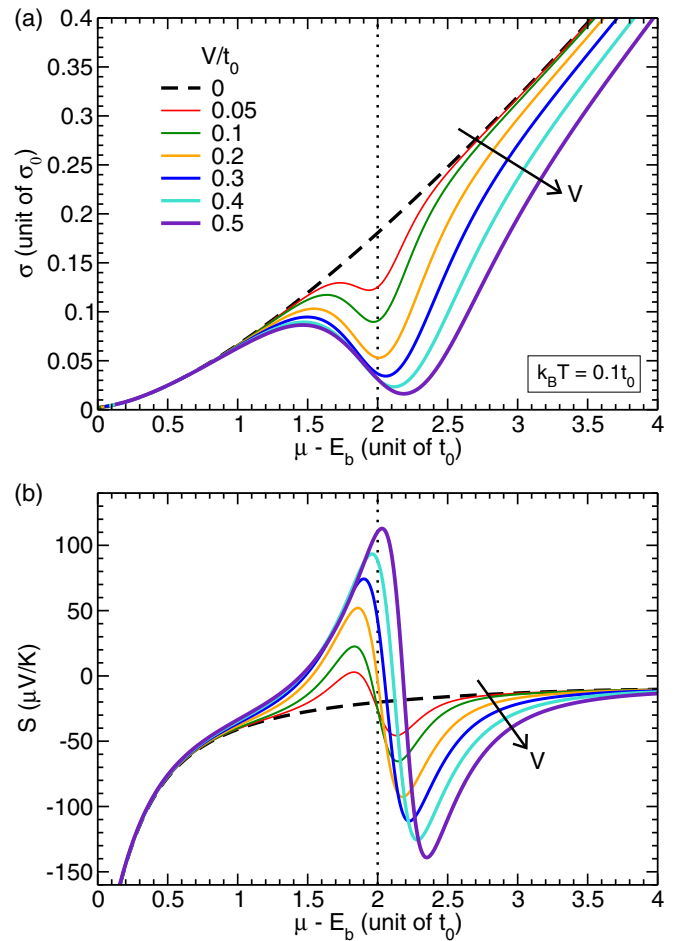


FIG. 4. (a) Electrical conductivity in units of $\sigma_0 = \frac{e^2 t_0 \tau_0}{a \hbar^2 \hbar}$ against μ for various V , $E_l - E_b = 2t_0$, and $k_B T = 0.1t_0$ (approximately room temperature). The reference case ($V = 0$) is the dashed black line. The flat band position is marked by a dotted black line. (b) Seebeck coefficient in $\mu V/K$.

within a large energy region around the resonance (shaded area on Fig. 3), this does not bode well indeed for the power factor. There is, however, a silver lining: by creating a dip in the Drude weight, the resonant band also introduces steep variations. Therefore, we expect the Seebeck coefficient to be boosted around the resonance and, since it is squared in the power factor, we can still hope that this effect will compensate the loss in conductivity and enhance the power factor.

In order to find out if this is true or not, we now present some results for the transport coefficients, giving special attention to comparisons between the power factor with and without resonance.

Setting the resonant band position at $E_l - E_b = 2t_0$, we investigate the effect of the hybridization amplitude V . We show in Fig. 4 the electrical conductivity (in units of $\sigma_0 = \frac{e^2 t_0 \tau_0}{a \hbar^2 \hbar}$) and the Seebeck coefficient (in $\mu V/K$) against the chemical potential μ , for several values of V . The temperature is set at $k_B T = 0.1t_0$, which corresponds to room temperature for $t_0 \approx 0.25$ eV (this is typically the case in SrTiO_3 [45], for instance). The resonant band position is marked by a dotted black line. As V is turned on from the reference case (dashed black line), the conductivity is suppressed near the resonant

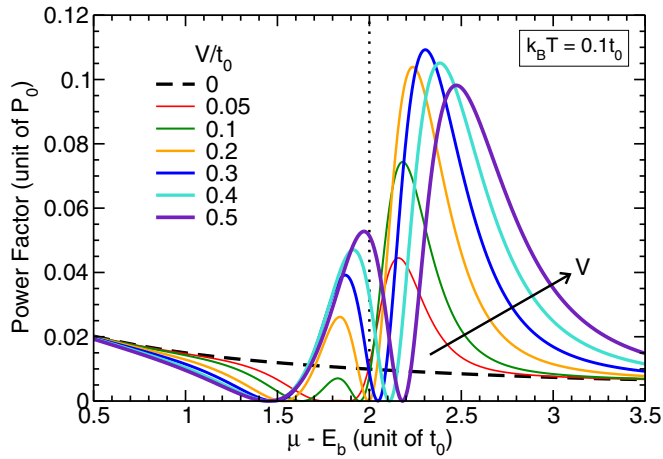


FIG. 5. The power factor in units of $P_0 = \frac{k_B^2 t_0 \tau_0}{a\hbar^2 \hbar}$ against μ for various V , $E_l - E_b = 2t_0$, and $k_B T = 0.1t_0$ (approximately room temperature). The reference case ($V = 0$) is the dashed black line. The flat band position is marked by a dotted black line.

band. As for the Seebeck coefficient, there is a boost on each side of the resonance and a change of sign for high enough values of V . The sign change is very interesting, because we are still in the conduction band. This might prove extremely useful for materials in which n -type doping is possible but p -type is difficult, or vice versa. The boost in the Seebeck coefficient is typically comparable or greater than the decrease in the electrical conductivity, so we expect the power factor (in which the Seebeck coefficient appears squared) to get boosted.

The power factor is plotted in Fig. 5 in units of $P_0 = \frac{k_B^2 t_0 \tau_0}{a\hbar^2 \hbar}$ for the same values of V , E_l , and T . There is a boost above and below the resonant band for high enough values of the hybridization, which confirms that hybridization plays a central role in resonant enhancement of the thermoelectric properties. Also, notice that the power factor is suppressed when the Fermi level is located inside the resonant band, unlike the mechanism in which the TDF is proportional to the carrier density. There appears to be an optimal value of V around $0.3t_0$, for which the power factor is an order of magnitude higher than its reference value at $\mu - E_b \approx 2.3t_0$. As this optimal value is not very dependent on the resonant band position, we set $V = 0.3t_0$ to discuss the influence of the other parameters, namely, the resonant band position E_l and the temperature T .

Turning our attention to the influence of the resonant band position E_l , we show the power factor against μ in Fig. 6 for $k_B T = 0.1t_0$ and three different band positions ($E_l - E_b = t_0$, $2t_0$, and $3t_0$, marked by dotted vertical lines), along with the reference (dashed black line). It is manifest that the closest the resonant band is to the center of the conduction band, the more boosted the power factor is. This makes sense: close to the center, the Drude weight is higher (see Fig. 3) and so the drop created by the resonant band is steeper. In fact, if the flat band lies outside the conduction band (below E_b), then the transport properties are the same as those of the reference case. Therefore, to achieve a significant boost of the power factor, the resonant band must be located well within the conduction band. This runs counter to the advice of Mahan and Sofo [18] to have a background DOS as small as possible. Of course, a resonant band located too far from the edge of the conduction

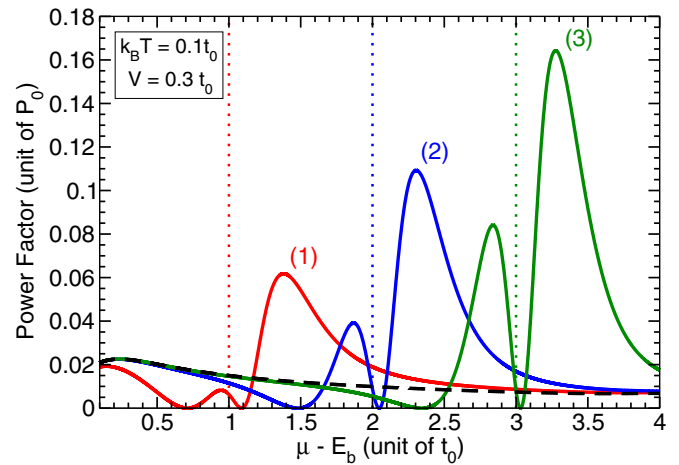


FIG. 6. The power factor in units of $P_0 = \frac{k_B^2 t_0 \tau_0}{a\hbar^2 \hbar}$ against μ for $V = 0.3t_0$, $k_B T = 0.1t_0$ (approximately room temperature), and $E_l - E_b = t_0$ (1), $E_l - E_b = 2t_0$ (2), and $E_l - E_b = 3t_0$ (3). The flat band position in each case is marked by a dotted line. The reference case ($V = 0$) is the dashed black line.

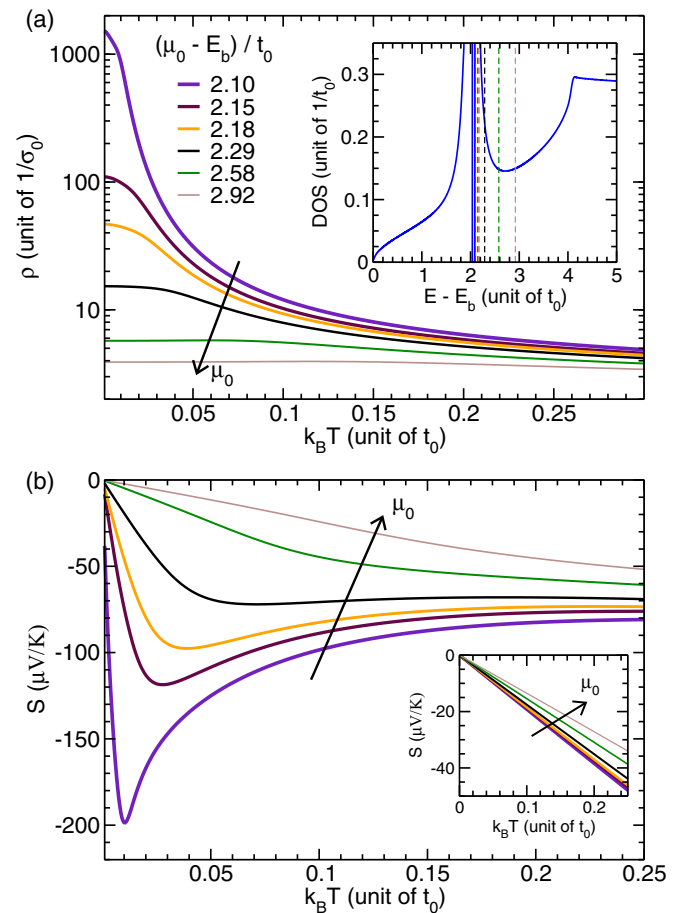


FIG. 7. (a) The resistivity in units of $\frac{1}{\sigma_0} = \frac{a\hbar^2 \hbar}{e^2 t_0 \tau_0}$ and logarithmic scale against the temperature for $V = 0.3t_0$, $E_l - E_b = 2t_0$, and six different electron densities. Each density is labeled by the chemical potential at $T = 0$ K, μ_0 , shown in the inset with the DOS. (b) The Seebeck coefficient in $\mu V/K$ against the temperature, with the reference case shown in the inset for the same μ_0 . Notice the different scales for the Seebeck coefficient.

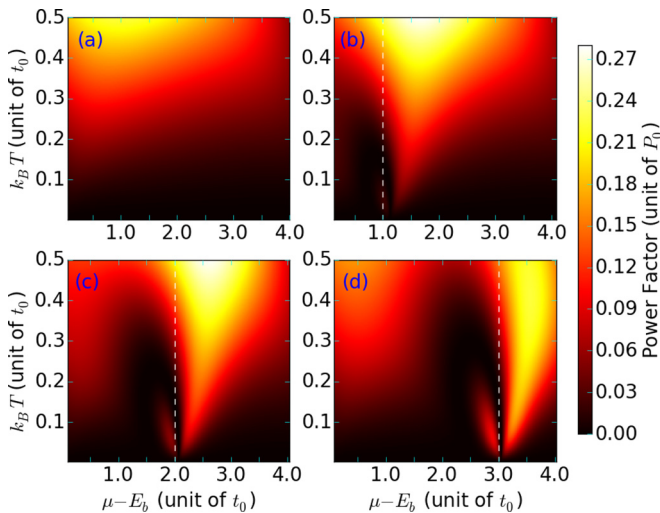


FIG. 8. Color map of the power factor in units of P_0 on the (μ, T) plane for the reference case $V = 0$ (a) and the resonant case $V = 0.3t_0$ with $E_l - E_b = t_0$ (b), $E_l - E_b = 2t_0$ (c), and $E_l - E_b = 3t_0$ (d). The dashed white lines mark the position of the flat band.

band would be inaccessible with reasonable doping, so the optimal location for the resonant level might be the result of a compromise.

We show in Fig. 7 the resistivity ρ (in log scale and units of $1/\sigma_0$) and the Seebeck coefficient against the temperature for six electron densities, each labeled by the chemical potential at $T = 0$ K, μ_0 , shown in the inset of panel (a). As the temperature changes, the electron density is fixed but the chemical potential varies. The reference case is shown in the inset for the Seebeck coefficient. Due to the heavy nature of the states near the resonance, the resistivity displays a metal-insulator transition as μ_0 draws closer to the resonant level. It is informative to study the behavior of the Seebeck coefficient as this metal-insulator transition takes place. Comparing the reference and resonant cases, the Seebeck coefficient is not only boosted but also displays a very different and nonstandard behavior, exhibiting a minimum at various temperatures if μ_0 is close enough to the resonance. It is important to keep in mind that such a structure may emerge from the distortion of the Drude weight caused by the presence of a resonant band.

In order to get an overview of the power factor with respect to the chemical potential and the temperature, we plot in Fig. 8 a color map of the power factor on the (μ, T) plane in the reference case $V = 0$ (a) and the resonant case $V = 0.3t_0$ with $E_l - E_b = t_0$ (b), $E_l - E_b = 2t_0$ (c), and $E_l - E_b = 3t_0$ (d). From Fig. 8(a), significantly increasing the power factor in the reference case requires going to temperatures as high as 1200 K (assuming $t_0 \approx 0.25$ eV). However, if a resonant band is present [Figs. 8(b)–8(d)], the region of high power factor is dragged down to much lower temperatures, a process that is more efficient the closer the resonant band is to the center of the conduction band.

In summary, we showed that it is possible to boost the power factor by introducing resonant states. We went over the mechanisms found in the literature about how resonant levels can enhance thermoelectric transport. To clarify the physical picture, the crucial role of hybridization, and the influence of the relevant physical parameters, we used a minimal tight-binding model featuring an extended conduction band hybridized with a heavy flat band. In contrast to the scenarios usually proposed, the presence of the resonant band was shown to introduce a significant dip in the Drude weight or, equivalently, in the transport distribution function and thus to suppress the conductivity. However, the strong variations of the transport distribution function lead to a boost in the Seebeck coefficient and overcompensate the conductivity reduction. This competition allows for a large increase in the power factor. We determined that a significant boost requires that the hybridization is sufficiently high (typically 30% of the hopping), that the resonant band is not located too close to the conduction band edge, and that the Fermi level is located near, but not inside, the resonant band. This new understanding of the mechanism by which resonant levels may influence thermoelectric transport opens the door to more sophisticated studies investigating, for instance, the effects of the density of resonant states, the anisotropy of the orbitals, and the nature of the hybridization (on-site or not, with multiple atoms, etc.). As our tight-binding model is compatible with the description of more complicated band structures and can easily accommodate the presence of disorder, it constitutes the basis from which such further studies can be carried out, hopefully leading to a better understanding of resonant doping.

-
- [1] X. Zheng, C. Liu, and Q. Wang, *Renew. Sustainable Energy Rev.* **32**, 486 (2011).
- [2] M. H. Elsheikh, D. A. Shnawah, M. F. M. Sabri, S. B. M. Said, M. H. Hassan, M. B. A. Bashir, and M. Mohamad, *Renew. Sustainable Energy Rev.* **30**, 337 (2014).
- [3] H. J. Goldsmid, *Introduction to Thermoelectricity* (Springer, Berlin, 2010).
- [4] D. Rowe, *CRC Handbooks of Thermoelectricity* (CRC Press, Boca Raton, FL, 1995).
- [5] X. Zhang and L.-D. Zhao, *J. Materiomics* **1**, 92 (2015).
- [6] M. G. Kanatzidis, *Chem. Mater.* **22**, 648 (2010).
- [7] A. J. Minnich, M. S. Dresselhaus, Z. F. Ren, and G. Chen, *Energy Environ. Sci.* **2**, 466 (2009).
- [8] C. J. Vineis, A. Shakouri, A. Majumdar, and M. G. Kanatzidis, *Adv. Mater.* **22**, 3970 (2010).
- [9] G. J. Snyder and E. S. Toberer, *Nat. Mater.* **7**, 105 (2008).
- [10] L. D. Hicks and M. S. Dresselhaus, *Phys. Rev. B* **47**, 12727 (1993).
- [11] L. D. Hicks and M. S. Dresselhaus, *Phys. Rev. B* **47**, 16631 (1993).
- [12] P. Pichanusakorn and B. Prabhakar, *Mater. Sci. Eng., R* **67**, 19 (2010).
- [13] J. P. Heremans, Proc. XXXIV Int. School Semicond. Compd. **108**, 609 (2005).
- [14] M. Dresselhaus, G. Chen, M. Tang, R. Yang, H. Lee, D. Wang, Z. Ren, J.-P. Fleurial, and P. Gogna, *Adv. Mater.* **19**, 1043 (2007).

- [15] L. D. Hicks, T. C. Harman, X. Sun, and M. S. Dresselhaus, *Phys. Rev. B* **53**, R10493(R) (1996).
- [16] R. Venkatasubramanian, E. Siivola, T. Colpitts, and B. O'Quinn, *Nature (London)* **413**, 597 (2001).
- [17] H. Ohta, S. Kim, Y. Mune, T. Mizoguchi, K. Nomura, S. Ohta, T. Nomura, Y. Nakanishi, Y. Ikuhara, M. Hirano *et al.*, *Nat. Mater.* **6**, 129 (2007).
- [18] G. D. Mahan and J. O. Sofo, *Proc. Natl. Acad. Sci. USA* **93**, 7436 (1996).
- [19] J. P. Heremans, B. Wiendlocha, and A. M. Chamoire, *Energy Environ. Sci.* **5**, 5510 (2011).
- [20] J. P. Heremans, V. Jovovic, E. S. Toberer, A. Saramat, K. Kurosaki, A. Charoenphakdee, S. Yamanaka, and G. J. Snyder, *Science* **321**, 554 (2008).
- [21] S. A. Nemov and Y. I. Ravish, *Phys.-Usp.* **41**, 735 (2008).
- [22] C. M. Jaworski, V. Kulbachinskii, and J. P. Heremans, *Phys. Rev. B* **80**, 233201 (2009).
- [23] Q. Zhang, B. Liao, Y. Lan, K. Lukas, W. Liu, K. Esfarjani, C. Opeil, D. Broido, G. Chen, and Z. Ren, *Proc. Natl. Acad. Sci. USA* **110**, 13261 (2013).
- [24] G. Tan, W. G. Zeier, F. Shi, P. Wang, G. J. Snyder, V. P. Dravid, and M. G. Kanatzidis, *Chem. Mater.* **27**, 7801 (2015).
- [25] Q. Zhang, H. Wang, W. Liu, H. Wang, B. Yu, Q. Zhang, Z. Tian, G. Ni, S. Lee, K. Esfarjani *et al.*, *Energy Environ. Sci.* **5**, 5246 (2012).
- [26] J. Li, X. Liu, Y. Li, S. Song, F. Liu, and W. Ao, *J. Alloys Compd.* **600**, 8 (2014).
- [27] D. Rowe, V. L. Kuznetsov, L. A. Kuznetsova, and G. Min, *J. Phys. D: Appl. Phys.* **35**, 2183 (2002).
- [28] J. Zhou, Z. Sun, X. Cheng, and Y. Zhang, *Intermetallics* **17**, 995 (2009).
- [29] X. H. Yang, *J. Alloys Compd.* **594**, 70 (2014).
- [30] D. J. Singh, *Phys. Rev. B* **81**, 195217 (2010).
- [31] H. Peng, J.-H. Song, M. G. Kanatzidis, and A. J. Freeman, *Phys. Rev. B* **84**, 125207 (2011).
- [32] D. Parker and D. J. Singh, *Phys. Rev. B* **82**, 035204 (2010).
- [33] X. Yang, X. Qin, D. Li, J. Zhang, C. Song, Y. Liu, L. Wang, and H. Xin, *J. Phys. Chem. Solids* **86**, 74 (2015).
- [34] N. W. Ashcroft and N. D. Mermin, *Solid State Physics* (Saunders, Philadelphia, 1976).
- [35] J.-H. Lee, J. Wu, and J. C. Grossman, *Phys. Rev. Lett.* **104**, 016602 (2010).
- [36] J. Yang, L. Xi, W. Qiu, L. Wu, X. Shi, L. Chen, J. Yang, W. Zhang, C. Uher, and D. J. Singh, *npj Comput. Mater.* **2**, 15015 (2015).
- [37] J. Zhou, R. Yang, G. Chen, and M. S. Dresselhaus, *Phys. Rev. Lett.* **107**, 226601 (2011).
- [38] C. Jeong and M. S. Lundstrom, *J. Appl. Phys.* **111**, 113707 (2012).
- [39] D. I. Bilc, G. Hautier, D. Waroquiers, G.-M. Rignanese, and P. Ghosez, *Phys. Rev. Lett.* **114**, 136601 (2015).
- [40] D. I. Bilc, C. G. Floare, L. P. Zârbo, S. Garabagiu, S. Lemal, and P. Ghosez, *J. Phys. Chem. C* **120**, 25678 (2016).
- [41] Y. Pei, H. Wang, and G. J. Snyder, *Adv. Mater.* **24**, 6125 (2012).
- [42] Y. Pei, X. Shi, A. LaLonde, H. Wang, L. Chen, and G. J. Snyder, *Nature (London)* **473**, 66 (2011).
- [43] Z. Zhong, Q. Zhang, and K. Held, *Phys. Rev. B* **88**, 125401 (2013).
- [44] Z. Zhong, P. Wissgott, K. Held, and G. Sangiovanni, *Europhys. Lett.* **99**, 37011 (2012).
- [45] G. Bouzerar, S. Thébaud, C. Adessi, R. Debord, M. Apreutesei, R. Bachelet, and S. Pailhès, [Europhys. Lett. (to be published)], [arXiv:1702.0275](https://arxiv.org/abs/1702.0275).
- [46] D. J. Scalapino, S. R. White, and S. Zhang, *Phys. Rev. B* **47**, 7995 (1993).
- [47] W. Kohn, *Phys. Rev.* **133**, A171 (1964).
- [48] A. J. Millis and S. N. Coppersmith, *Phys. Rev. B* **42**, 10807 (1990).
- [49] G. Bouzerar and R. Bouzerar, *New J. Phys.* **13**, 023002 (2011).